Pion single charge exchange angular distributions at $T_\pi = 48$ MeV

M. J. Leitch*
TRIUMF, Vancouver, British Columbia, Canada V6T 2A3
and Los Alamos National Laboratory, Los Alamos, New Mexico 87545

H. W. Baer, J. D. Bowman, M. D. Cooper, E. Piasetzky, U. Sennhauser,† and H. J. Ziock
Los Alamos National Laboratory, Los Alamos, New Mexico 87545

F. Irom* and P. B. Siegel
Arizona State University, Tempe, Arizona 85287

M. A. Moinester
Tel Aviv University, Ramat-Aviv, Israel
(Received 6 May 1985)

Angular distributions for pion single charge exchange to the isobaric analog state were measured for ^{39}K and ^{48}Ca at $T_\pi = 48$ MeV. The cross sections on ^{39}K and ^{48}Ca exhibit a less deep minimum at zero degrees than was seen previously on ^{15}N. The large-angle ^{39}K cross sections are roughly equal to those for ^{15}N, while the 0° to 60° ^{48}Ca cross sections are approximately four times larger. The extrapolated zero-degree center-of-mass cross sections are 2.7 ± 1.0 μb/sr for ^{15}N, 12 ± 5 μb/sr for ^{39}K, and 110 ± 25 μb/sr for ^{48}Ca, and the angle-integrated cross section for ^{39}K is 557 ± 65 μb. The large back-angle cross sections for ^{39}K are attributed to strong quadrupole contributions to the isobaric analog state transition.

INTRODUCTION

The study of pion-nucleus reactions has been of great interest due to the strong energy dependence of the pion-nuclear interaction over the 3-3 resonance region. As these reactions are followed down to low pion energies (below 100 MeV), the interaction becomes decreasingly Δ dominated and other aspects of the reaction mechanism become increasingly important and available for study. Near 50 MeV a nearly complete forward-angle cancellation between the π-nucleon single charge exchange (SCX) s- and p-wave amplitudes, with a rapid energy dependence, causes the SCX reaction in nuclei to be sensitive to nuclear-medium effects. The manifestation of this cancellation in a nucleus depends on the relative weighting of the s- and p-wave parts of the interaction, which can be altered by various nuclear-medium effects, e.g., Lorentz-Lorenz correlations, Pauli blocking, and absorption.

Recently the first observation for a nucleus of this deep minimum at forward angles was reported for the reaction ^{15}N$(\pi^+,\pi^0)^{15}$O (IAS) at 48 MeV.[1] This angular distribution for the transition to the isobaric analog state (IAS) in ^{15}O exhibits a deep minimum at zero degrees analogous to that in the π-nucleon charge exchange and is fundamentally different from the same pion-nucleus reaction near the Δ-resonance energy (Fig. 1). This minimum has also been seen in the ^{7}Li$(\pi^+,\pi^0)^7$Be (IAS) zero-degree excitation function.[2] This can be interpreted as an indication that light nuclei, for which the strong cancellation of the fundamental amplitudes persists, are relatively transparent to pions near 50 MeV. It has also been interpreted as evidence for Lorentz-Lorenz correlations[1,3] or Pauli blocking.[4] In order to investigate the A dependence of the nuclear-medium effects on this cancellation phenomena, we have made new measurements on medium mass nuclei. Presented here are angular distributions at 48 MeV for the reactions ^{39}K$(\pi^+,\pi^0)^{39}$Ca (IAS) and ^{48}Ca$(\pi^+,\pi^0)^{48}$Sc (IAS).

EXPERIMENT

The experiment was done using the LAMPF π^0 spectrometer[5] on the low-energy pion (LEP) channel[6] at the Clinton P. Anderson Meson Physics Facility (LAMPF) of the Los Alamos National Laboratory. The spectrometer was set in its one-post configuration (horizontal scattering plane) with all three conversion planes in place and a distance from target to first conversion plane of 54 cm. In this configuration an angular range of 25 deg is covered for one setting. This range has been divided into two angle bins for each setting. The photon detectors were set for a central opening angle of 93.72° corresponding to 50 MeV π^0s. The π^0 energy resolution, which is dominated by target effects, especially at backward angles, varied between 5.5 and 7 MeV (FWHM).

The ^{39}K target consisted of four rectangular pieces of natural potassium (93.3% ^{39}K), each about 260 mg/cm^2, enclosed in an aluminum frame with 0.113 mm aluminum windows. For the forward-angle measurements all four pieces were used with an air space between each in order to improve the energy resolution according to the compensation technique.[5] Near 90° only two pieces were used and at the largest angle all four were used. The targets were tilted with respect to the beam in order to face more

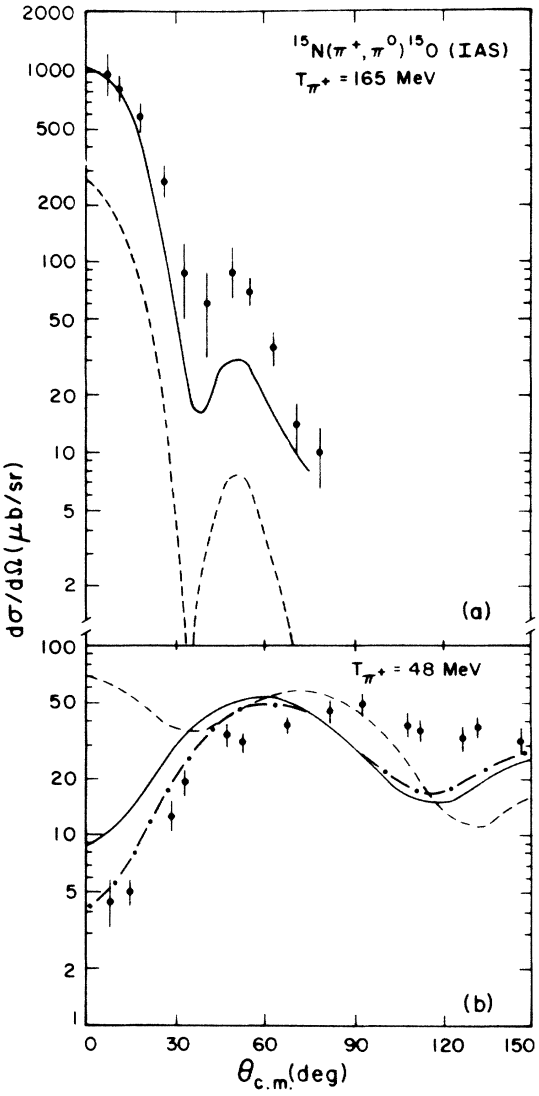

FIG. 1. Angular distributions for IAS transition $^{15}N(\pi^+,\pi^0)^{15}O$ at $T_\pi=165$ MeV and $T_\pi=48$ MeV. The curves shown are optical model calculations by Siciliano (Ref. 13). The solid curve includes a correlation term. The dot-dashed curve has a correlation term and an absorption term. The dashed curve has neither.

nearly normal to the spectrometer. The ^{48}Ca targets (94.5% isotopic purity) consisted of four pieces, each about 100 mg/cm^2 thick. A 439 mg/cm^2 CH_2 target, along with a background target of 495 mg/cm^2 ^{12}C, was used to check the normalization and calibration of the spectrometer by measuring the $\pi^-p\rightarrow\pi^0n$ reaction cross section at 155° and 100 MeV.

The LEP channel was run with a flux between 1.2 and $1.6\times10^7\pi^+$/sec and a momentum bite of 3% (FW) for the π^+ measurements, and a flux of 7×10^6 π^-/sec and momentum bite of 1% (FW) for the π^- measurement ($\pi^-p\rightarrow\pi^0n$).

The data were normalized using a Monte Carlo simulation of the spectrometer to determine its acceptance and the scintillator activation technique to determine the pion flux. The pion flux relative to a toroidal pickup loop around the primary proton beam was determined from the known activation cross sections[7] in a Pilot-B scintillator by measuring the induced β activity ($\tau_{1/2}\sim20.33$ min) from the reaction $^{12}C(\pi^\pm,\pi n)^{11}C$.

A Monte Carlo simulation of the spectrometer was used to obtain the geometrical acceptance. Various nongeometrical efficiencies were determined by the following methods. The photon conversion efficiency was calculated from analytic fits to conversion efficiency data. Results obtained from two different sources (Refs. 5 and 8) were in excellent agreement. The loss of photons due to absorption in the target and in the 3.8 cm of CH_2 which

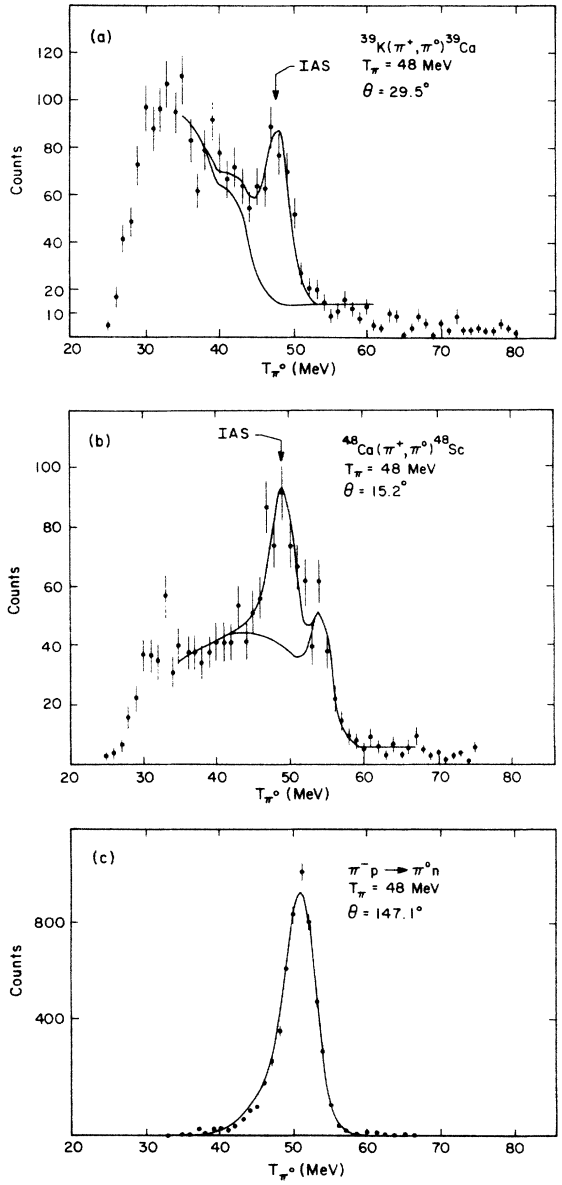

FIG. 2. Spectra at $T_\pi=48$ MeV for (a) $^{39}K(\pi^+,\pi^0)$ at 29.5°, (b) $^{48}Ca(\pi^+,\pi^0)$ at 15.2°, and (c) $\pi^-p\rightarrow\pi^0n$ at 147.1°. The curves represent the fits to the spectra. For ^{39}K and ^{48}Ca these include the IAS, excited states, the continuum, and a flat background as described in the text.

was located on the front of each photon detector was calculated using the tables of Hubbell.[9] Wire chamber efficiencies were evaluated by observing the fraction of events in which only two out of the three wire chambers in a conversion module registered the track. The loss in efficiency due to analysis constraints was determined by careful inspection of the loss of good events in the tails of each distribution which had a constraint imposed upon it. The nonstatistical uncertainties in the normalization were roughly 10%. The cross section determined following this procedure of $\pi^- p \rightarrow \pi^0 n$ at an incident pion energy of 100 MeV, resulting in a 52 MeV π^0 at 155°, agreed to within the ±6% variation between different phase-shift solutions.

Yields for the IAS transition were extracted from the π^0 energy spectrum by fitting with the Monte Carlo generated line shape using a maximum likelihood method.[10] The energies of the IAS peak, other states, and the breakup threshold were fixed by kinematics. The fitting uncertainty was adjusted to account for the possibility of including or not including excited states. A flat background representing charge exchange from air and random events was determined from the kinematically forbidden region above the IAS energy. The fitting uncertainty also includes contributions due to the uncertainty in this background shape. Figure 2 shows several typical spectra along with representative fits. There is good agreement between the experimental line shape and that from the Monte Carlo, especially for $\pi^- p \rightarrow \pi^0 n$. For the back-angle ^{39}K data where the instrumental resolution is broader and the first excited state group at 2.5 MeV may be excited, the well-determined line shape and fixed loca-

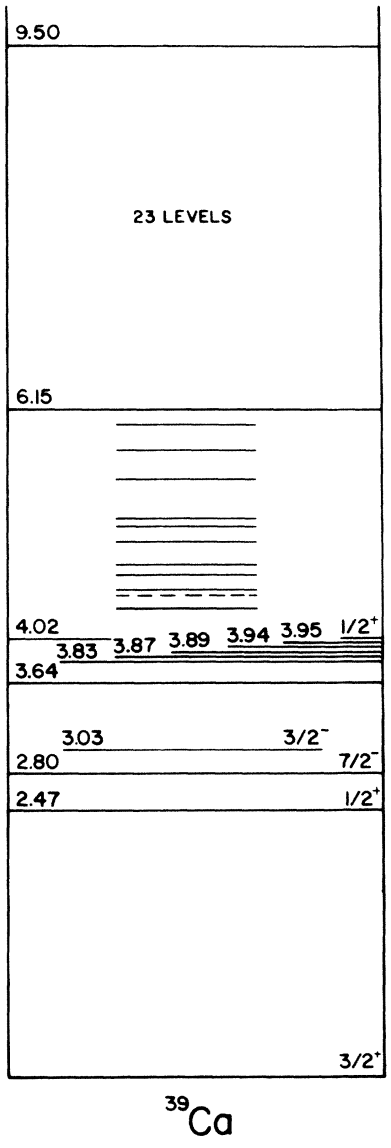

FIG. 3. The level scheme for ^{39}Ca (Ref. 20).

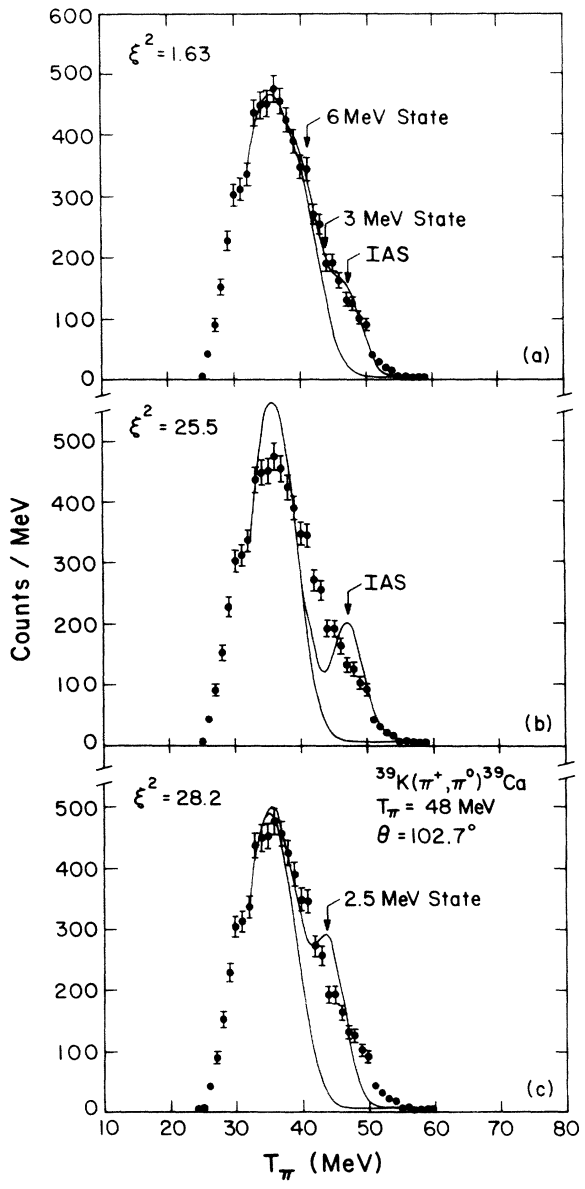

FIG. 4. Three fits to the 48 MeV $^{39}K(\pi^+,\pi^0)^{39}Ca$ spectrum at 102.7° (a) with the IAS, an excited state group at 2.5 MeV, and an excited state group at 6 MeV; (b) with the IAS alone; and (c) with the 2.5 MeV group alone. The energies of the states are fixed by kinematics and the line shape is from a Monte Carlo calculation.

tion in energy of the IAS peak are essential. The level scheme for the residual ^{39}Ca nucleus is shown in Fig. 3. In the fitting to the data, excited state groups at 2.5 MeV, corresponding to the first three excited states between 2.5 and 3 MeV, and at 6 MeV corresponding to the many states above 3.6 MeV, were considered. The $\frac{1}{2}^+$ state at 2.5 MeV, which is strongly excited in the (^{3}He,t) reaction,[11] was also found to be important here. In Fig. 4, fits to the energy spectrum with one or more states included are shown, illustrating the level of separation of the IAS from excited states. Shown are a fit with the IAS, the 2.5 MeV, and the excited state group at 6 MeV included; then fits with each of the IAS and the 2.5 MeV group alone. When the 2.5 MeV group alone is fit a clear excess of counts above it in energy corresponding to the IAS can be seen. Similarly, a fit with the IAS alone shows a clear need for excited state strength. These fits with either state alone give a ξ^2 about 15 times worse than the fit with both IAS and excited states, where ξ^2 is the goodness of fit parameter analogous to χ^2 in least squares fitting. For the reaction ^{48}Ca(π^+,π^0)^{48}Sc, where the analog state is in the continuum at an excitation energy of 6.7 MeV, the possibility of contributions from underlying discrete states cannot be excluded. In (p,n) reactions on ^{48}Ca at similar momentum transfer[12] a 1^+ state at 2.5 MeV excitation and some strength at excitation energies near and above the IAS is seen. However, since the coupling of the pion to the nucleus is, in principle, different than that for the proton, it is uncertain whether similar strength is present in pion SCX. In our analysis we have assumed a smooth background under the IAS peak and have included variations in its level and shape in the quoted uncertainties.

DATA AND DISCUSSION

In Table I we present the center-of-mass cross sections for a pion laboratory energy of 48 MeV. Also included are the ^{15}N cross sections which were previously published,[1] but only in graphical form. Complete angular distributions were obtained for ^{15}N and ^{39}K, but for ^{48}Ca only the range 0°—70° was covered because of background uncertainties (see Fig. 5). In addition to the relative uncertainties shown, there are the previously mentioned absolute uncertainties of 10% for ^{39}K and ^{48}Ca. For ^{15}N the full uncertainty is included in the error bar for each point. The absolute uncertainties for ^{39}K and ^{48}Ca are dominated by the uncertainties in the activation cross sections used to determine the pion fluxes (±6.8%), by the photon conversion probability, and by the wire chamber efficiencies (each ±5%). Additional uncertainties come from the

TABLE I. (π^+,π^0) IAS cross sections at T_π=48 MeV in μb/sr.

	θ_{lab} (deg)	$d\sigma/d\Omega_{lab}$ (μb/sr)	$\theta_{c.m.}$ (deg)	$d\sigma/d\Omega_{c.m.}$[a] (μb/sr)
^{39}K	15.3	21.3 ± 3.2	15.4	21.1± 3.2
	29.5	35.4± 3.3	29.6	35.1± 3.2
	53.5	47.9± 4.0	53.7	47.6± 4.0
	69.3	32.6± 3.9	69.6	32.5± 3.9
	102.7	49.7± 5.1	103.0	49.8± 5.1
	118.5	59.3± 6.3	118.8	59.6± 6.3
	147.5	43.3±12.9	147.7	43.7±13.1
	162.0	47.9±14.2	162.1	48.4±14.4
^{48}Ca	15.2	120.1±23.8	15.3	119.1±23.6
	29.1	147.0±25.3	29.2	145.9±25.1
	52.3	187.1±36.3	52.5	186.1±36.1
	68.3	86.0±26.1	68.5	85.7±30.0
^{15}N	7.9	4.6± 1.3	8.0	4.5± 1.3
	14.6	4.9± 0.8	14.8	5.0± 0.8
	28.4	13.0± 2.6	28.7	12.7± 2.5
	33.3	19.4± 3.2	33.6	19.0± 3.1
	48.0	34.2± 4.7	48.5	33.6± 4.6
	53.0	31.0± 3.7	53.6	30.5± 3.6
	67.3	37.9± 3.2	68.0	37.5± 3.2
	81.7	44.3± 5.8	82.4	44.1± 5.7
	92.9	47.6± 6.5	93.7	47.7± 6.5
	107.7	37.0± 4.8	108.4	37.3± 4.8
	112.3	34.4± 4.7	113.0	34.7± 4.8
	127.0	30.9± 4.5	127.6	31.4± 4.5
	132.0	34.9± 4.5	132.6	35.5± 4.6
	146.6	29.4± 4.2	147.0	30.0± 4.3

[a]In addition to the uncertainties shown, there are absolute uncertainties of ±10% for ^{39}K and ^{48}Ca. For ^{15}N the full uncertainty is included for each data point.

reconstruction efficiency (±3%), the γ absorption (±2%), and the computer live time (±2%). The relative errors are determined by the statistics of each measurement and by systematic uncertainties involved in the fit to each peak.

We have determined angle-integrated and zero-degree extrapolated cross sections from these data by fitting them with Legendre polynomials in the scattering angle. The angle-integrated cross section for ^{15}N is 430±70 μb (from Ref. 1) and for ^{39}K is 557±65 μb. The extrapolated zero-degree cross sections are 2.7±1 μb/sr for ^{15}N, 12±5 μb/sr for ^{39}K, and 110±25 μb/sr for ^{48}Ca.

The cross sections are plotted in Fig. 5 along with optical model calculations using the computer program PIESDEX of Siciliano and Johnson.[13] The calculation contains several ρ^2 (second order in nuclear density) terms which represent absorption, short- and long-range correlations, Pauli blocking, and scattering through nonanalog intermediate routes. The FP84 phase shift solution of Arndt[14] was used to obtain the first order parameters. Pauli blocking effects were included by multiplying the imaginary terms of the first order isoscaler parameters by the Goldberger-Clementel-Villi form of the Pauli factor,[15] calculated with a Fermi momentum of 1.4 fm^{-1}. The second order includes s- and p-wave isoscaler parameters which were obtained from Table IV, set C, of Ref. 16, and a phenomological isovector p-wave term representing absorption.[1] These parameter values, in the notation of Ref. 12, are as follows:

$$\mathrm{Re}\bar{\lambda}_0^{(2)} = -0.106, \quad \mathrm{Im}\bar{\lambda}_0^{(2)} = 0.742 ,$$

$$\mathrm{Re}\lambda_0^{(2)} = 0.666, \quad \mathrm{Im}\lambda_0^{(2)} = 1.091 ,$$

$$\mathrm{Im}\lambda_1^{(2)} = -1.5 ,$$

and a Pauli suppression factor of 0.3. Both isoscaler and isovector Lorentz-Lorenz-Ericson-Ericson correlations are included with a strength (λ_{LLEE}) of 1.6 fm^{-1}. The nuclear densities used were generated from a Hartree-Fock calculation with a Skyrme III force.[17] Calculations are shown for only the valence density (ρ excess) and for $\rho_n - \rho_p$. These two types of densities are described in Ref. 18 where, for ^{39}K on resonance, the choice between them is shown to be very important. The use of ρ excess gives better agreement with the ^{48}Ca data than $\rho_n - \rho_p$, but is

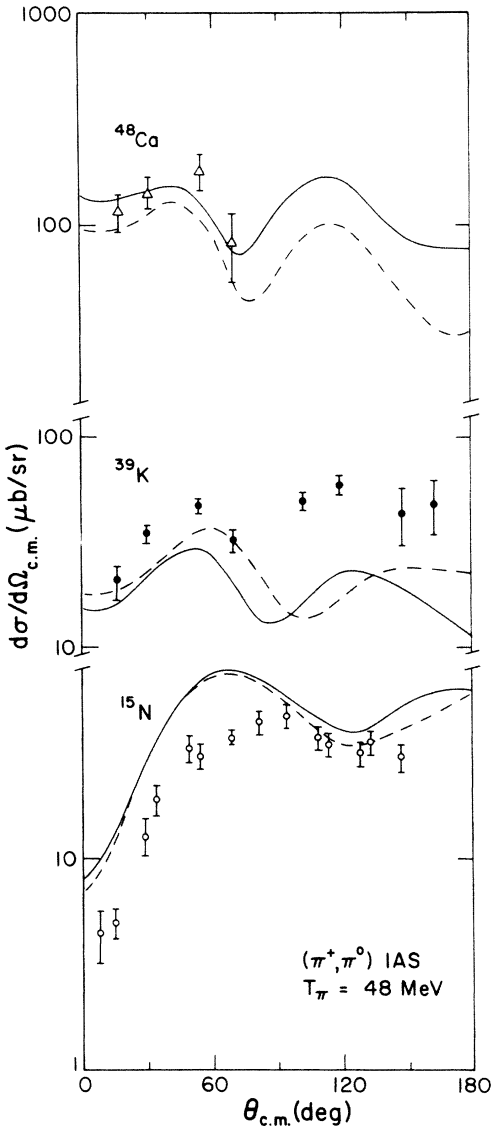

FIG. 5. Angular distributions for the IAS transition for SCX in ^{15}N, ^{39}K, and ^{48}Ca. Two sets of calculations with PIESDEX (Ref. 13) are shown, both using densities derived from the Skyrme III model. The solid curves are calculations with ρ excess and the dashed curves are with $\rho_n - \rho_z$ (see Ref. 18).

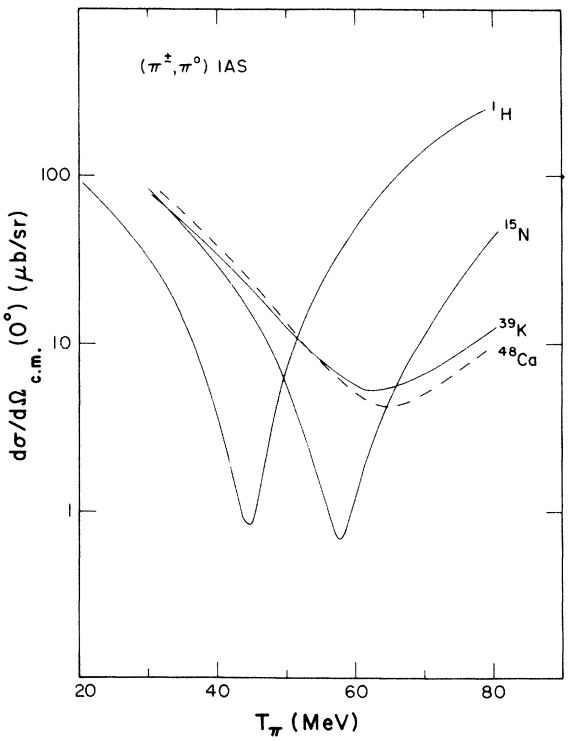

FIG. 6. Zero-degree excitation function predictions from PIESDEX (Ref. 13) for pion SCX on various nuclear targets showing the predicted A dependence of the location and width of the minimum.

slightly worse for ^{39}K. The shape is qualitatively correct but the predicted magnitude for ^{39}K is low, especially at backward angles, where the ^{39}K and ^{15}N cross sections are roughly equal in size. Also we see that the forward-angle parts of the measured cross sections for the ^{39}K and ^{48}Ca do not show as deep a minimum as ^{15}N does. We have used the same optical model program to suggest a likely explanation. In Fig. 6 are shown the calculated excitation functions at zero degrees for SCX on these nuclei. The same parameters which were used above for the 48 MeV calculation are assumed to be energy independent and used here for illustrative purposes. The $\pi^-p\rightarrow\pi^0n$ shown is from the FP84 phase shifts of Arndt.[14] Several general trends are predicted: the energy at which the minimum occurs moves up in energy with A and is broader and less deep for larger A. Either or both of these trends can explain the observed data at 48 MeV. It may be that if the medium-weight nuclei are measured at a slightly higher energy, these angular distributions will show a deep forward-angle minimum also. Another aspect of this phenomenon is shown in Fig. 7, where the A dependence of the zero degree cross section for a variety of nuclei and five energies is shown. For energies 100 MeV and above the data fall on a line which is representative of black disc scattering (see Ref. 19). At 48 MeV this is no longer true. These data show a sharp dip in the A dependence of the forward angle cross section, reflecting the rapidly varying elementary amplitude that manifests itself differently in nuclei as a function of A.

Several general features of the non-zero-degree and integrated cross sections, where delicate cancellations do not

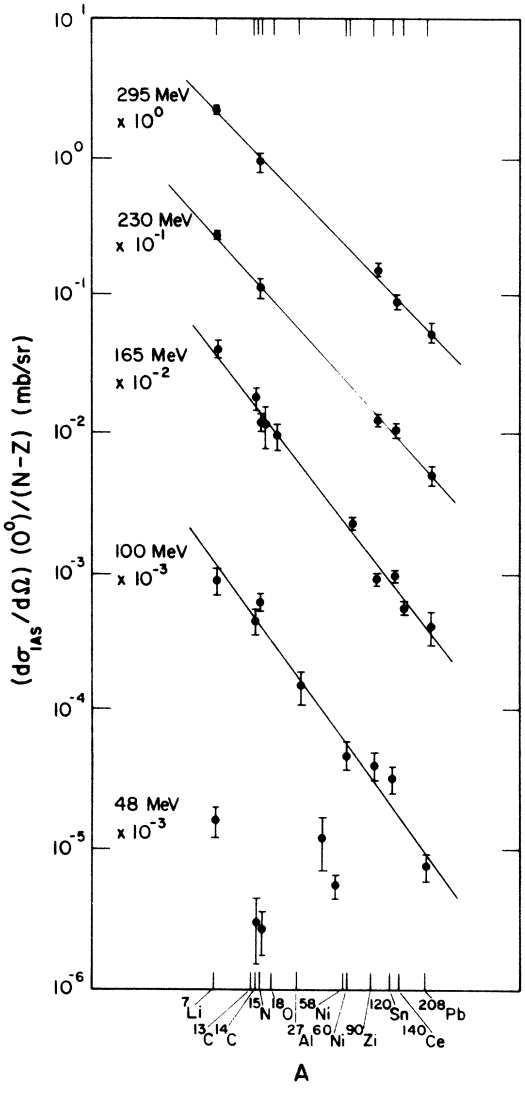

FIG. 7. A dependence of the zero-degree cross section illustrating the breakdown at 48 MeV of the simple A dependence seen at 100 MeV and higher. Reference 19 contains the data at 100 MeV and above and describes the lines through the data. The 48 MeV ^{7}Li data point is from Ref. 2 and the 48 MeV ^{14}C data point is from Ref. 21.

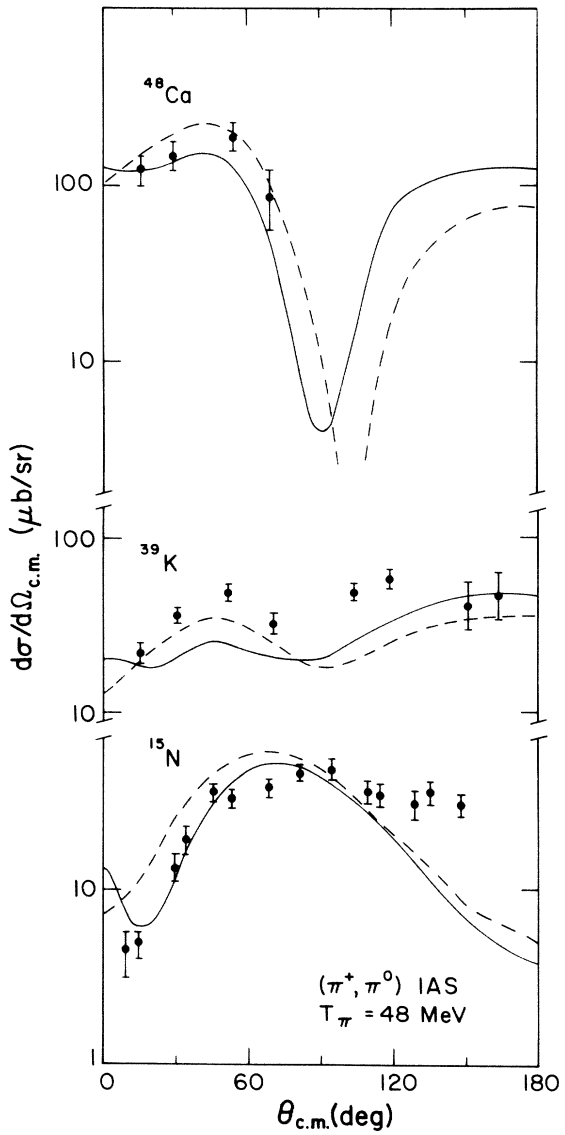

FIG. 8. DWIA calculations using the procedure of Kaufmann and Gibbs (Ref. 4) compared to the data on ^{15}N, ^{39}K, and ^{48}Ca. The solid curves are calculations with the full optical potential and the dashed curves are with $V_{opt}=0$.

play such an essential role, can be seen. The ^{39}K cross section is roughly equal to the ^{15}N cross section and is about $\frac{1}{4}$ that of ^{48}Ca. This implies that the valence neutron in ^{39}K contributes as strongly as does that in ^{15}N, while only half of the eight valence neutrons in ^{48}Ca effectively contribute to the analog reaction cross section. The PIESDEX calculation shown underpredicts ^{39}K, yet does quite well for ^{48}Ca. This appears to be a shortcoming of the model because the comparison with ^{48}Ca implies that the reduction in the cross section due to medium effects is just strong enough, while comparison with ^{39}K suggests it is too strong. Also, uncertainties in the nuclear densities may contribute to this failure.

In Fig. 8 we show the results of a DWIA calculation using the procedure of Kaufmann and Gibbs.[4] The main ingredients for this calculation are the transition density, transition operator, and the distorted waves. Transition densities were obtained from wave functions generated by a Woods-Saxon potential with the strength adjusted to fit the experimental value of the valence-nucleon binding energy and the range determined from the nuclear size. In Fig. 9 are shown the resulting transition densities and also the analogous Skyrme III (Ref. 17) densities, which are very similar. The resulting differential cross sections differ only slightly, as can be seen by comparing Fig. 8 to Fig. 10. The transition operator is of the form

$$t_{\rm op}=\lambda_0+\lambda_1\mathbf{k}\cdot\mathbf{k}'+\lambda_{\rm SF}\sigma\cdot(\mathbf{k}\times\mathbf{k}')\ ,$$

where k and k′ are the incoming and outgoing pion momenta, and the λ's are determined from the free charge exchange reaction (π^-p$\rightarrow\pi^0$n) and include angle and frame transformations. The first two terms can induce non-spin-flip transitions (monopole, quadrupole, . . .) and the last term, spin-flip transitions.

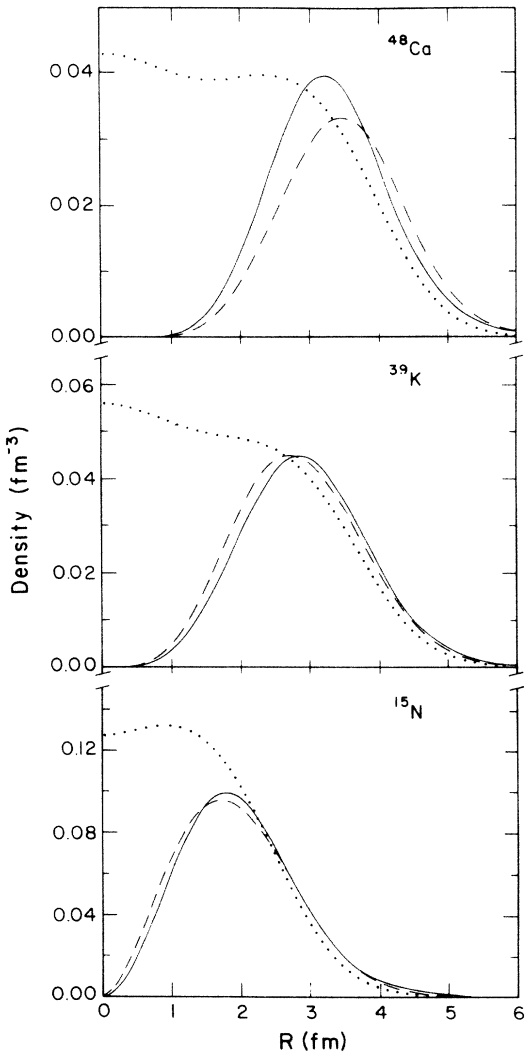

FIG. 9. Transition densities for ^{15}N, ^{39}K, and ^{48}Ca. The solid curves are the Woods-Saxon densities as described in the text, the dashed curves are ρ excess obtained from the Skyrme III model, and the dotted curves are the core density divided by A.

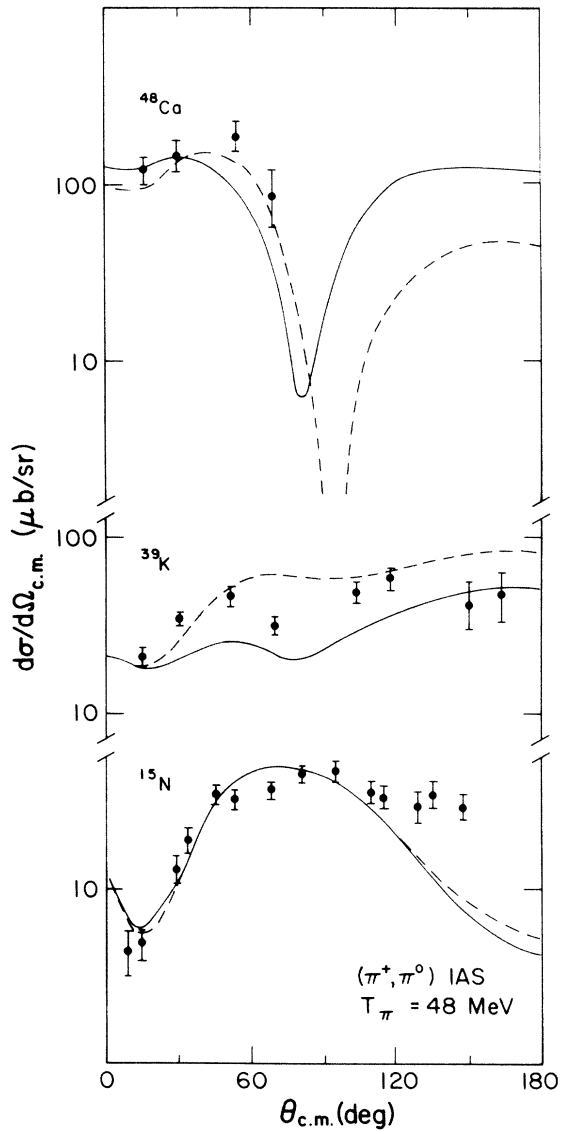

FIG. 10. DWIA calculations for the full optical potential and Skyrme III densities. The solid curve is for ρ excess and the dashed curve is for $\rho_n-\rho_p$.

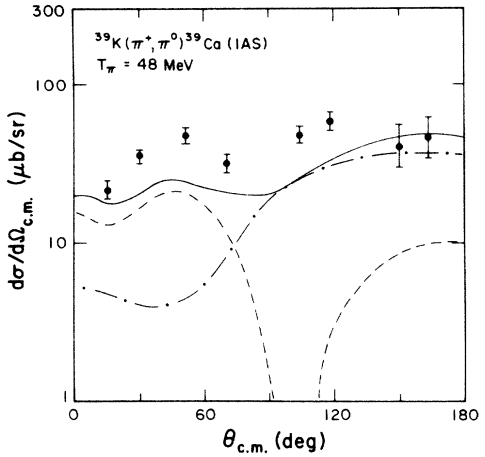

FIG. 11. DWIA calculations for the full optical potential and Woods-Saxon densities. The dashed curve is the monopole, the dot-dashed the quadrupole, and the solid curve is the sum of monopole and quadrupole.

For each nucleus, two curves corresponding to the use of different distorted waves are presented in Fig. 8. The dashed lines are a result of setting $V_{opt}=0$ (i.e., only the Coulomb potential) in generating the distorted waves, whereas the solid curves include the optical potential of Ref. 4. At low energies the imaginary part of this first-order optical potential is greatly reduced due to blocking effects, leading to increased transparency. This is demonstrated in the similarity between the two calculations, and their success supports the hypothesis that the nucleus is relatively transparent to low energy pions. In Fig. 10 DWIA calculations with Skyrme III densities are compared to the data. Two calculations are shown for each nucleus, one using ρ excess and one using $\rho_n-\rho_p$. Neither calculation gives significantly better agreement with the data and, as was also seen with PIESDEX, the difference between the resulting cross sections is very small compared to the factor of 13 (on resonance) of Ref. 18. This is due to the increased transparency at this energy and hence reduced sensitivity of the cross section to the density differences at the nuclear surface. Another feature of using the DWIA is the straightforward calculation of quadrupole transitions. In particular, for ^{39}K, quadrupole contributions become significant at back angles (Fig. 11) where the quadrupole form factor is large at this energy. Monopole calculations using the DWIA or PIESDEX are well below the data at back angles, and the discrepancy is greatly reduced by including these effects.

In conclusion, we have extended the measurement of 50 MeV SCX to the IAS to medium-weight nuclei. The deep forward-angle minimum seen for ^{15}N is not as pronounced for ^{39}K and ^{48}Ca. The ^{39}K cross sections at larger angles are roughly equal to those for ^{15}N while those for ^{48}Ca are about four times larger. The large backward-angle strength for ^{39}K, which cannot be predicted by monopole calculations, appears to be explained by a large quadrupole contribution to the IAS transition. The systematics of these cross sections with energy and with A are expected to yield information about the role of multinucleon effects in the SCX reaction. We expect that, since the nearly complete cancellation between s- and p-wave amplitudes occurs near 50 MeV, these sensitivities are enhanced. As more data become available, we may be able to isolate and study these multinucleon effects.

ACKNOWLEDGMENTS

We acknowledge the effective help of many people at Los Alamos National Laboratory and thank N. Auerbach, W. R. Gibbs, M. B. Johnson, and E. R. Siciliano for many illuminating discussions. This work was supported by the National Sciences and Engineering Council of Canada, the U. S. Department of Energy, and in part by the U.S.-Israel Binational Science Foundation.

*Present address: Los Alamos National Laboratory, Los Alamos, NM 87545.

†Present address: SIN, Swiss Institute for Nuclear Research, CH-5234 Villigen, Switzerland.

[1]M. D. Cooper, H. W. Baer, R. Bolton, J. D. Bowman, F. Cverna, N. S. P. King, M. Leitch, J. Alster, A. Doran, A. Erell, M. A. Moinester, E. Blackmore, and E. R. Siciliano, Phys. Rev. Lett. **52**, 1100 (1984).

[2]F. Irom, H. W. Baer, J. D. Bowman, M. D. Cooper, E. Piasetzky, U. Sennhauser, H. J. Ziock, M. J. Leitch, A. Erell, M. A. Moinester, and J. R. Comfort, Phys. Rev. C **31**, 1464 (1985).

[3]M. Ericson and T. E. O. Ericson, Ann. Phys. (N.Y.) **36**, 323 (1966); J. M. Eisenberg, J. Hufner, and E. J. Moniz, Phys. Lett. **47B**, 381 (1973).

[4]W. B. Kaufmann and W. R. Gibbs, Phys. Rev. C **28**, 1286 (1983).

[5]H. W. Baer, R. D. Bolton, J. D. Bowman, M. D. Cooper, F. H. Cverna, R. H. Heffner, C. M. Hoffman, N. S. P. King, J. Piffaretti, J. Alster, A. Doron, S. Gilad, M. A. Moinester, P. R. Bevington, and E. Winkelmann, Nucl. Instrum. Methods **180**, 445 (1981).

[6]R. L. Burman, R. L. Fulton, and M. Jakobson, Nucl. Instrum. Methods **131**, 29 (1975).

[7]B. J. Dropesky, G. W. Butler, C. J. Orth, R. A. Williams, M. A. Yates-Williams, G. Friedlander, and S. B. Kaufman, Phys. Rev. C **20**, 1844 (1979); G. W. Butler, B. J. Dropesky, C. J. Orth, R. E. L. Green, R. G. Korteling, and G. K. Y. Lam, *ibid.* **26**, 1737 (1982).

[8]D. I. Sober, private communication.

[9]J. H. Hubbell, U. S. Department of Commerce Report NSRDS-NBS 29, 1979.

[10]M. D. Cooper, H. W. Baer, J. D. Bowman, F. H. Cverna, R. H. Heffner, C. M. Hoffman, N. S. P. King, J. Piffaretti, J. Alster, A. Doron, S. Gilad, M. A. Moinester, P. R. Bevington, and E. Winklemann, Phys. Rev. C **25**, 438 (1982).

[11]J. J. Schwartz and B. A. Watson, Phys. Lett. **31B**, 198 (1970).
[12]B. D. Anderson, T. Chittrakarn, A. R. Baldwin, C. Lebo, R. Madey, R. J. McCarthy, J. W. Watson, B. A. Brown, and C. C. Foster, Phys. Rev. C **31**, 1147 (1985).
[13]M. B. Johnson and E. R. Siciliano, Phys. Rev. C **27**, 730 (1983); **27**, 1647 (1983); E. R. Siciliano, M. D. Cooper, M. B. Johnson, and M. J. Leitch (unpublished).
[14]R. A. Arndt, program SAID (Scattering Analysis Interactive Dialin), Virginia Polytechnic Institute and State University, 1984.
[15]R. H. Landau and M. McMillan, Phys. Rev. C **8**, 2094 (1973).
[16]K. Stricker, J. A. Carr, and H. McManus, Phys. Rev. C **22**, 2043 (1980).
[17]E. R. Siciliano and M. B. Johnson, private communication; M. Beiner, H. Flocard, Nguyen Van Giai, and P. Quentin, Nucl. Phys. **A238**, 29 (1975).
[18]N. Auerbach, M. B. Johnson, A. Klein, and E. R. Siciliano, Phys. Rev. C **29**, 526 (1984).
[19]U. Sennhauser, E. Piasetzky, H. W. Baer, J. D. Bowman, M. D. Cooper, H. S. Matis, H. J. Ziock, J. Alster, A. Erell, M. A. Moinester, and F. Irom, Phys. Rev. Lett. **51**, 1324 (1983).
[20]P. M. Endt and C. Van Der Leun, Nucl. Phys. **A310**, 528 (1978).
[21]J. L. Ullman, P. W. F. Alons, J. J. Kraushaar, J. H. Mitchell, R. J. Peterson, R. A. Ristinen, J. N. Knudson, J. R. Comfort, H. W. Baer, J. D. Bowman, M. D. Cooper, D. H. Fitzgerald, F. Irom, M. J. Leitch, and E. Piasetzky, submitted to Phys. Rev. C.